analytical chemistry

pubs.acs.org/ac Article

Segmented Flow Strategies for Integrating Liquid Chromatography−Mass Spectrometry with Nuclear Magnetic Resonance for Lipidomics

Jiajun Lei, Rohit Mahar, Mario C. Chang, James Collins, Matthew E. Merritt, Timothy J. Garrett, and Richard A. Yost*

Cite This: *Anal. Chem.* 2023, 95, 1908−1915 Read Online

ACCESS | Metrics & More | Article Recommendations | Supporting Information

ABSTRACT: Building an accurate lipid inventory relies on coordinated information from orthogonal analytical capabilities. Integrating the familiar workflow of liquid chromatography (LC), high-resolution mass spectrometry (HRMS), and tandem mass spectrometry (MS/MS) with proton nuclear magnetic resonance spectroscopy (^{1}H NMR) would be ideal for building that inventory. For absolute lipid structural elucidation, LC−HRMS/MS can provide lower-level structural information with superior sensitivity, while ^{1}H NMR can provide invaluable higher-order structural information for the disambiguation of isomers with absolute chemical specificity. Digitization of the LC eluent followed by splitting the microfractions into two flow paths in a defined ratio for HRMS/MS and NMR would be the ideal strategy to permit correlation of the MS and NMR data as a function of chromatographic retention time. Here, we report an active segmentation platform to transform analytical flow rate LC eluent into parallel microliter segmented flow queues for high confidence correlation of the MS, MS/MS, and NMR data. The practical details in implementing this strategy to achieve an integrated LC−MS−NMR platform are presented, including the development of an active segmentation technology using a four-port two-way valve to transform the LC eluent into parallel segmented flows for online MS analysis followed by offline segment-specific ^{1}H NMR and optimization of the detector response toward segmented flow. To demonstrate the practicality of this novel platform, it was tested using lipid mixture samples.

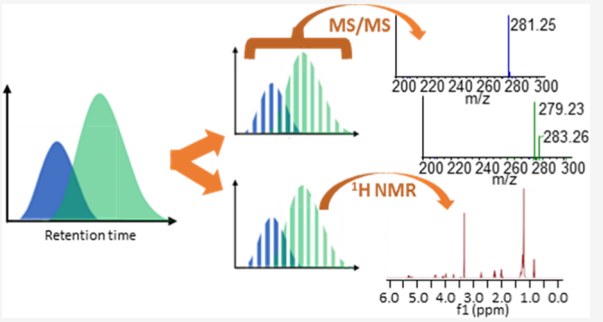

Merging nuclear magnetic resonance spectroscopy (NMR) into the classic liquid chromatography−mass spectrometry (LC−MS)-based lipidomics workflow would be ideal for lipid structural elucidation as the lipid isomeric themes that can be challenging for high-resolution mass spectrometry (HRMS)/MS alone can be resolved with diagnostic ^{1}H NMR chemical shift and split patterns,[1] and the advent of microcoil probes with capillary delivery of the sample to the microliter volume detection cell effectively addresses many of the issues regarding NMR sensitivity and sample handling.[2] However, NMR cannot operate on the LC−MS timescale as NMR is still less sensitive than MS. To decouple the HRMS/MS and ^{1}H NMR acquisition timescales, the chromatographic eluent can be digitized into bins and split into two parallel flow paths at a high enough frequency to preserve the separation efficiency. For typical analytical flow rate LC separations, a bin volume around a few microliters should provide 10 or more bins across each chromatographic peak. Then, correlation between orthogonal analytical information from MS and NMR can be achieved by sending one of those parallel flows for real-time HRMS/MS analysis while storing the other digitized flow for later selection of bins to be sent to a capillary flow cell for high mass sensitivity ^{1}H NMR. The digitization frequency and split ratio can be optimized based on LC, MS, and NMR parameters.

Traditional tube-based fraction collection could in principle perform this task as it can change position every second, and microvolume injectors could be configured to deliver a portion of the pooled fraction for MS analysis with the rest left in the collection vial for subsequent NMR analysis. Sumner et al. have employed fraction collection for peak-wide fractionation on targeted and well-resolved LC peaks, with the fraction collector triggered at predetermined retention times or based upon signal intensity at predetermined MS1 m/z values, with those selected based upon a previous LC/MS experiment.[3] A 96-well plate was used for offline solid-phase extraction solvent

Received: September 9, 2022
Accepted: December 27, 2022
Published: January 11, 2023

https://doi.org/10.1021/acs.analchem.2c03974
Anal. Chem. 2023, 95, 1908−1915

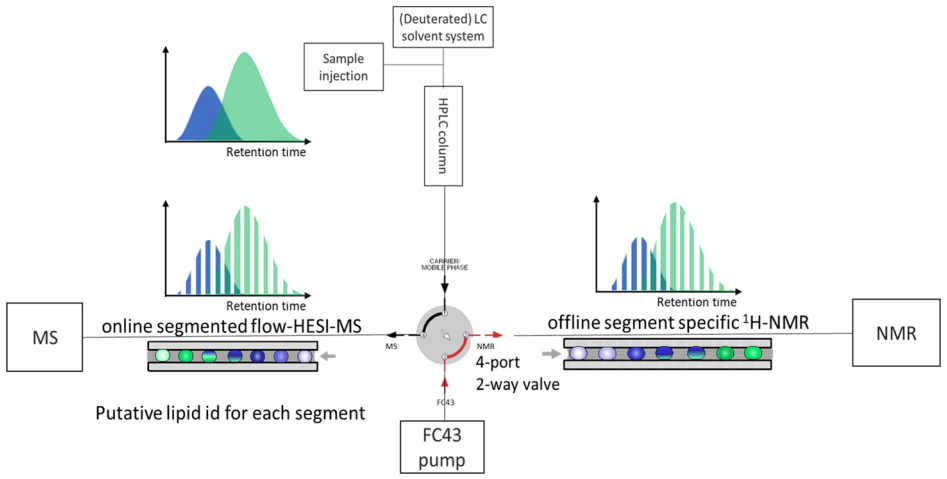

Figure 1. Active segmentation platform to transform continuous LC into parallel segmentation for online HESI-MS analysis and offline segment-specific ^{1}H NMR.

exchange, and a 192-position rack was used for online collection of the deuterated mobile phase eluent into 1.7 mm NMR tubes.[3] However, there are significant limitations to this approach. First, for lipid mixtures with coeluting isomeric species, the MS1 ion will not allow fractionation of such species. Second, variation in the retention time between one LC/MS run to select retention times of interest and a subsequent LC/MS run to collect fractions can lead to errors in fraction selection. Finally, limits on the number of collection tubes and their cost make traditional fraction collection a poor choice for integrating LC/MS with NMR.

Here, we report the use of zero-dispersion segmented flow as an ideal strategy for storing a large number (thousands) of eluent fractions for subsequent NMR analysis by queueing them in capillary tubing separated by plugs of an immiscible carrier phase; the manipulation of these digitized segments can be achieved via pumping and other microfluidic means.[4] To transform a continuous chromatogram into a segmented chromatogram, passive segmentation using a tee or Y-junction would appear to be an appealing high-frequency digitization strategy as segmentation is automatically generated and it is possible to modulate the plug formation dynamics by adjusting either the immiscible phase properties and flow rate or the dimensions of the tee or Y-junction.[5,6] Following passive segmentation, microfluidics channels fabricated on plastic chips have also been developed to split segments in a defined ratio so that the daughter plugs can be sent for different purposes.[7]

Although passive segmentation followed by splitting seems promising for LC−MS−NMR applications, several intrinsic difficulties limit its practicality. First, the applications of passive segmentation are mostly found in the nanoflow and microflow rate range, resulting in picoliter to nanoliter segments.[8] Such small segments would be a challenge to handle even with capillary flow NMR probes, which typically have volumes in the microliter range (although a custom-built nanoliter probe designed for a lower strength magnet has been reported[9]). Furthermore, at such low flow rates, passive segmentation dynamics are sensitive to variations in LC pump flow and pressure as well as to changes in the mobile phase gradient. The variations in segment sizes would pose problems for MS analysis and for matching to the NMR probe volume. Additionally, given that the mass loading capacity for capillary and microbore LC columns is in the low μg range, the available mass for individual species would be in the low ng range or below, which represents the best NMR mass sensitivity achieved so far using microliter detection volume microcoil probes.

Moving to an analytical LC column increases the sample loading capacity and improves the flow rate consistency, but the higher flow rate poses challenges for passive segmentation. Although passive segmentation in the microliter regime has been demonstrated using a 1/16 in. i.d. tee junction and optical detection,[10] the carrier phases used were highly viscous oleic acid and silicone oil, which are neither electrospray ionization (ESI)-MS nor NMR silent, and splitting of the segments into two parallel flow paths was not demonstrated. Thus, an alternative (active) segmentation platform to transform the analytical LC flow rate eluent into microliter zero dispersion segmented flow with segment splitting is desired for interfacing LC−MS and NMR.

In this work, we report an active parallel segmentation platform using a four-port two-way valve operating at analytical LC flow rates and microliter segmentation regime, as shown in Figure 1. Perfluorotributylamine (FC43) is chosen as the carrier phase due to its immiscibility with the lipid-containing eluent, plus its lipophobicity, nonionizability under ESI,[11,12] and transparency to ^{1}H NMR. The parallel segmentation profiles are defined by the flow rates of the LC eluent and FC43 into the valve inlet ports and the valve rotor switching frequency and duty cycle. Data from the online HRMS/MS analysis of one segmented chromatogram can be used to direct the subsequent offline segment-specific ^{1}H NMR on only those segments containing unknowns of interest.

We selected segment volumes of 2 to 4 μL to match the Protasis microcoil probe detection cell volume. To achieve 8 to 12 segments over a typical 10 to 30 sec wide chromatographic peak for MS analysis (and the same number for NMR analysis), flow rates of 240 μL/min for both the LC and the FC43 carrier phase were used, requiring the valve to switch between the LC eluent and the carrier phase at a frequency of ~1 Hz. Based upon those settings, MS and data-dependent MS/MS parameters were optimized, including ion source parameters. This optimization ensured that the overall segmentation profile could be extracted from the MS and data-dependent MS/MS scan data, and allowed segments of

https://doi.org/10.1021/acs.analchem.2c03974
Anal. Chem. 2023, 95, 1908−1915

interest to be located for ^{1}H NMR. Although the current platform focuses on a specific flow rate, active segmentation based on valve switching could be employed across a wide range of flow rate regimes, provided that the tubing connections can withstand the increase in backpressure at higher flow rates.

EXPERIMENTAL SECTION

Active Segmentation Platform Assembly. The active segmentation hardware platform was built using commercially available products. 1/16 in. o.d. and 500 μm i.d. perfluoroalkyl (PFA) tubing and matching zero dead volume connection unions were purchased from IDEX (Oak Harbor, WA) for segmented flow transfer and storage tubing. A VICI Cheminert four-port two-way valve (C2-2344, Valco, Houston, TX) with the associated control module was digitally controlled by a 0−5 V square wave synthesized by a 15 MHz function generator (33120A, Agilent) to define the driver cycle frequency and duty cycle. Porting of the valve follows the principle that the LC effluent as the disperse phase and FC43 as the carrier phase are pumped into opposite inlet ports, as shown in Figure 1.

MS Optimization for Segmented Flow. Extensive optimization of Heated ESI (HESI) ion source conditions for segmented flow was carried out on a TSQ ACCESS MAX triple quadrupole mass spectrometer (Thermo Fisher, San Jose, CA, USA). The experimental setup and optimization details can be found in Figure S1. The optimized source settings were then validated on Thermo Q-Exactive and Q-Exactive HF orbitrap mass spectrometers in full scan mode as they employ the same HESI source. TopNddms^2 scan mode optimization for segmented flow is demonstrated using passive segmentation. FC43 and 1 ppm DG (18:1/18:1 9Z) lipid standard sample solutions were pumped at 9 μL/min into two arms of the same Y junction, and the generated segmented flow was collected and transferred through the PFA tubing into the ion source. The settings for a trapping type mass analyzer such as an orbitrap (including maximum ion injection time and AGC target) can affect the scan speed; thus, fundamental characterization of the effect of these settings on the segmented flow response was performed as well.

LC-Segmentation-MS Analysis. A Vanquish UHPLC connected to a Thermo Q-Exactive mass spectrometer was employed for LC-segmentation-MS experiments. A PC [18:0/18:2 (9Z, 12Z)] standard and an egg PC mixture were used to demonstrate the active segmentation performance. Given the flow rate at 240 μL/min, LC separation was carried out on a Phenomenex core−shell C18 column (100 × 2.1 mm, 1.7 μm, part no. 00D-4475-AN, Torrance, CA) with the column oven temperature set to 50 °C. A binary mobile phase system of A (H_2O + 0.1% FA) and B (MeOH + 0.1% FA) was used to achieve the following gradient for optimum separation of the egg PC mixture: 0−0.5 min, 60% B; 0.5−2 min, 60−95% B; 2−17 min, 95% B; 17−17.5 min, 95−60% B; 17.5−20 min, 60% B. The LC eluent is connected to the valve port no. 4, while the FC43 is pumped into the valve port #2, as shown in Figure S2. The valve is set to switch at 0.5 or 0.714 Hz corresponding to 4 and 2.8 μL segmentation, respectively. For MS analysis, the optimized HESI source parameters for segmented flow at 240 μL/min were adopted, and the S-Lens RF level was kept at 50. The orbitrap mass analyzer was operated at a resolution of 35,000 in full-scan mode (scan range: m/z 120−1200; AGC target: 1×10^6).

NMR Spectroscopy. For the Protasis CapNMR probe (Marlboro, MA, USA) microcoil sensitivity test, the experimental setup and parameters can be found in Figure S3. For proof-of-concept PFA tubing through cryoprobe ^{1}H NMR experiments, the hardware setup schematic and experiment details can be found in Figure S4.

Data Processing. MS raw files were analyzed using Thermo Xcalibur Qual Browser 3.0.63. ^{1}H NMR spectra were processed using MestReNova v14.0.1-23284 (Mestrelab Research S.L.) software. ^{1}H NMR spectra were Fourier transformed with an exponential line-broadening factor of 0.3 Hz and zero filling to 64k points, and automatically phased and spline baseline corrected.

RESULTS AND DISCUSSION

As noted above, we selected a flow rate of 240 μL/min with 2−4 μL segments for the current platform to match the Protasis microcoil probe detection cell volume and to collect 8−12 segments over a typical 10−30 sec chromatographic peak. This flow rate is low enough to meet back pressure limits for the fingertight PFA tubing as well as pump pressure limits for the viscous FC43, and the separation efficiency was maintained by using a 2.1 mm wide column. For our platform, 2−4 μL segmentation of a working flow rate at 240 μL/min represents a valve cycling frequency between 0.5 and 1 Hz, which is not demanding. While the valve itself can switch at higher frequencies, it may generate too much mechanical heat for the valve body to dissipate rapidly, and this could shorten its lifetime.

Optimization of the valve active segmentation was performed first. Ideally, with the carrier phase and disperse phase flow rates set equal and the valve duty cycle set to 50:50, two identical segmentation profiles would be observed, with one steady and smooth flow rate minimally affected by valve rotation. Intriguingly, the upstream pump flow rate inconsistency and the downstream flow resistance mismatch can affect the instantaneous flow rate coming out of the outlet ports and therefore the collected segmentation profile. For example, for online ESI-MS and offline ^{1}H NMR, the flow resistances downstream of the two valve outlet ports are not equal due to differences in transfer and storage tubing lengths and the small diameter ESI needle compared to that of the PFA tubing. This was observed to lead to sudden changes in flow rates inside the PFA tubing in sync with valve rotation. This effect was corrected for by simply attaching a piece of fused silica tubing matching the additional flow resistance of the ESI needle to the end of the storage tubing.

The optimization of HESI source condition for segmented flow was next undertaken to determine whether rapid ion intensity drop and rise at segment interfaces would be observed, producing an ideal "on and off" pattern. The optimum HESI gas flow and temperature should be low enough to not affect segmentation while still in the liquid flow path but high enough to rapidly evaporate FC43 once it reaches the ESI needle tip. In addition, the optimum HESI parameters should provide a balance between efficient desolvation and ionization of analytes in the sample segments and preservation of segmentation integrity within the liquid flow path. Optimum conditions were achieved with the vaporizer temperature set to a typical value (360 °C) while the auxiliary gas is kept off. If too much heat is transferred to the liquid flow path, it could disrupt segmentation integrity due to significant changes in viscosity or even volatilize the liquid

https://doi.org/10.1021/acs.analchem.2c03974
Anal. Chem. 2023, 95, 1908−1915

while within the flow path. Since all instruments used the same HESI source, the optimized source parameters can be reliably transferred across different instruments, as shown in Figure S5. The EIC profiles acquired on a TSQ triple quadrupole mass spectrometer and on QE and QE-HF mass spectrometers (with 2 μL segments pumped at 240 μL/min) each resemble the expected square wave pattern, demonstrating robustness in source parameter transferability.

Scan mode optimization for segmented flow was focused on the orbitrap TopNddms^2 mode[13] due to its capability to rapidly acquire HRMS and ddms^2 scans. The scan mode optimization process was demonstrated using passive segmentation, as illustrated in Figure S6. A balance between the number of full scans and ddms^2 scans is made, given the instrument scan speed and per-segment allowed time, which is determined by the segment size and flow rate. With an appropriate ddms^2 threshold set, only low total ion intensity full scans are captured across the FC43 segment. The full scan intensity at the segment edge is lower than in the middle of the segment, which is likely due to the ESI-specific transient equilibration behavior since no ions are being formed during the FC43 segment. Thus, at least one full scan in the middle of the segment is required. For segment counting purposes, the TopNddms^2 response for segmented flow does not resemble the on and off pattern as the isolation quadrupole filters the sampled ion current during the MS/MS scans. Instead, we relied on the actual ion injection time over TopNddms^2 full scans only as its profile is complementary to the rapid TIC fluctuation pattern, as shown in Figure 2. Due to the limited

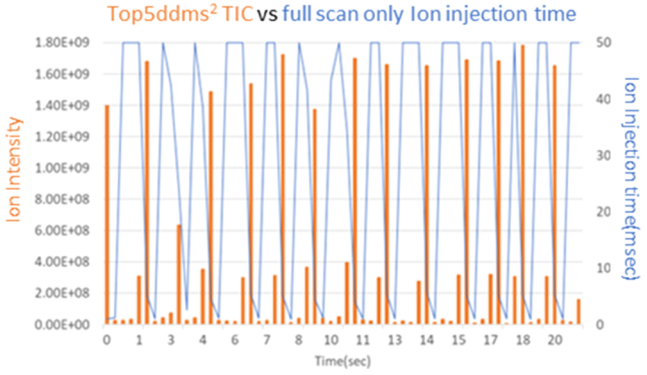

Figure 2. Full scan actual ion injection time profile can be used to distinguish and count segments from the TopNddms^2 TIC response for segmented flow. The orange bars are the total ion current from the Top5ddms^2 full scans (RS@30,000) and MS/MS scans (RS@15,000), and the blue trace shows the ion injection time for the Top5ddms^2 full MS scans only.

time available per segment, however, the ion abundance-based ion selection algorithm for fragmentation allows only species with high ion intensities to be selected for the subsequent MS/MS scan, potentially missing lipid species of interest at lower abundance. Faster scan speed orbitrap instruments and alternative data-dependent MS/MS acquisition, such as global targeted ddms^2 approach to import in silico-generated lipid precursor ion library as inclusion list,[14] are strategies that could improve the lipid ion selection efficiency.

To demonstrate the performance of the active segmentation platform, the egg PC mixture separation eluent at 240 μL/min was segmented at 0.714 Hz; the resultant segmented chromatogram for seven selected lipids species over an 8 min elution window is shown in Figure 3B (the egg PC mixture individual species profiles can be found in Figures S7 and S8). This can be compared to the continuous (unsegmented) chromatogram in Figure 3A. Comparing the chromatograms validates the active segmentation platform performance under real LC conditions. For better visualization of the segmented chromatogram and comparison with the continuous chromatogram, Figure S9 shows the extracted ion chromatograms for just two of these lipid species, PC (36:2) and PC (38:4). Thirty segments (each 2.8 μL) are observed over the 0.7 min elution window of these two lipids (recall that there are another 30 segments adjacent to each of these that were split to the flow path for subsequent NMR analysis). The separation efficiency is preserved as the same chromatographic resolution 1.0 is estimated from the continuous and segmented extracted ion chromatogram of PC (36:2); the normalized intensities of the extracted ion chromatogram are comparable, indicating no sensitivity is lost due to segmentation and the FC43 is not interfering with the eluent segment ionization process.

While MS data can help inform the selection of segments for ^{1}H NMR analysis, MS/MS data can provide even better insight into isomer separation by LC and therefore more informed selection of segments for ^{1}H NMR analysis. This is illustrated in Figure 4 when the orbitrap is scanning in the parallel reaction monitoring MS/MS mode with the dwell time spent evenly on the precursor ions at m/z 786.60 and 810.60, corresponding to the $[M + H]^+$ ions of PC (36:2) and PC (38:4), respectively. Both of these lipid species can include multiple isomers, and MS/MS data can permit their differentiation. In this case, MS/MS fragment ions are observed corresponding to loss of the fatty acyl chains indicative of several isomers, including m/z 281.25 for PC (18:1_18:1), m/z 279.23 for PC (18:0_18:2), m/z 307.26 for PC (16:0_20:2), and m/z 303.23 for PC (18:0_20:4). The extracted isomer-differentiating fatty acyl chain fragment ion intensity profiles shown in Figure 4 clearly show the elution profile of the four closely eluting isomeric species identified at the fatty acyl chain level. The high digitization of the segmentation platform guarantees the separation efficiency is preserved, with typically 20 segments across each isomer's LC peak. This permits the MS/MS-guided intelligent selection of segments for ^{1}H NMR analysis; the interpretation of the NMR data will be made much easier by selecting segments that contain a single isomer or a simple mixture. With the large number of segments preserving the chromatographic separation efficiency and LC/MS and MS/MS data on the individual segments, one can far more intelligently select specific segments to provide the cleanest NMR spectra compared to peak wide fraction collection that has been achieved with previous LC/MS/NMR platforms.

The Protasis capillary microcoil probe was initially targeted for segment-specific ^{1}H NMR, and we determined its limit of detection to be in the 150−200 ng range at 11.7 T magnetic field strength, assuming a total of 64 scans is used for acquisition, as shown in Figure 5. The ^{1}H NMR chemical specificity using the microcoil probe was also validated against all isomeric themes, as shown in Figures S10−S13. Unfortunately, the Protasis capillary probe is not optimal for loading segmented flow, as the fused silica flow path does not favorably wet with the perfluorinated liquid. Although perfluoro-octylsilane coating of the fused silica feedline and the flow cell have been demonstrated as a potential solution to

https://doi.org/10.1021/acs.analchem.2c03974
Anal. Chem. 2023, 95, 1908−1915

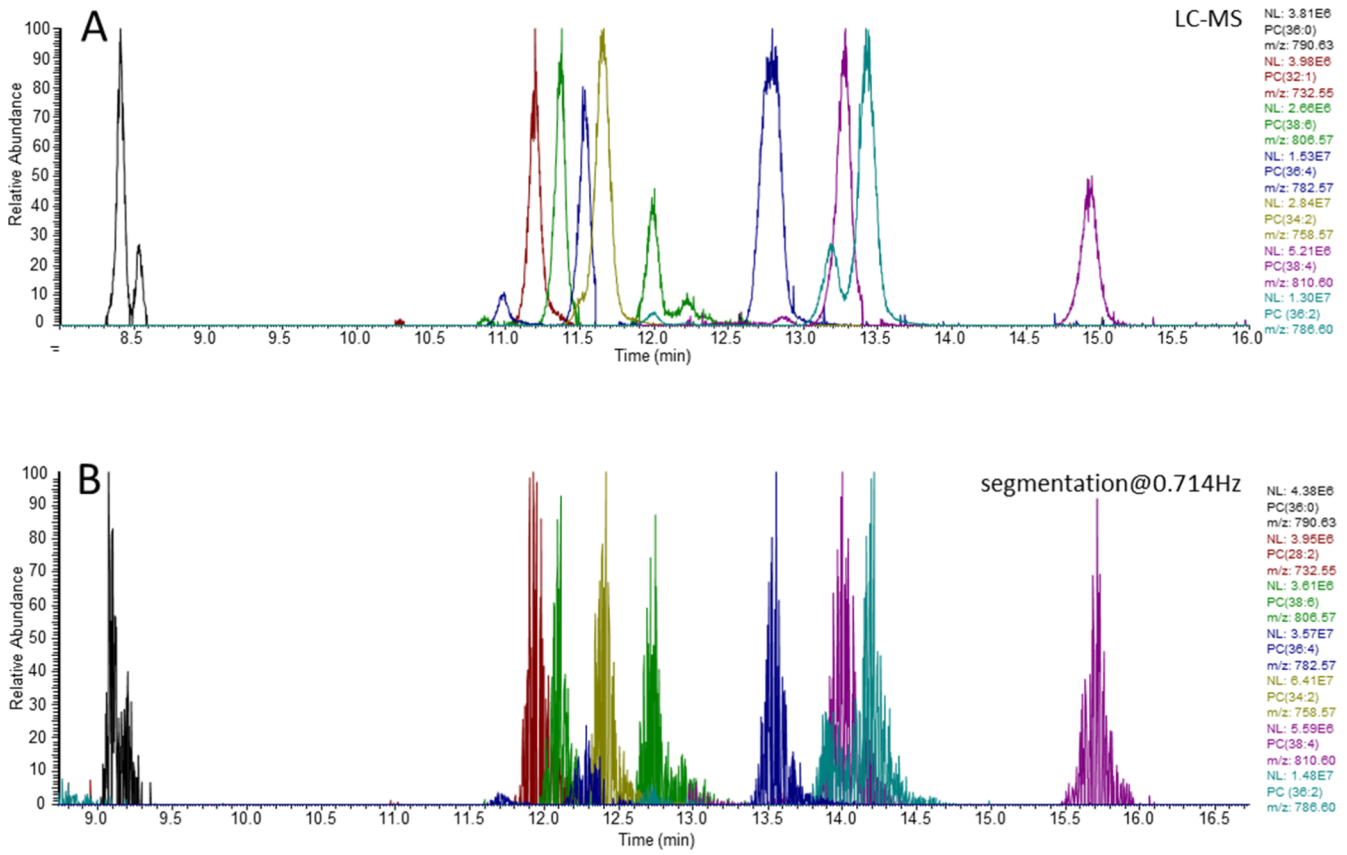

Figure 3. Segmented chromatogram (B) compared to the continuous, unsegmented chromatogram (A) for seven different m/z values to show the active segmentation performance. Flow rate is at 240 μL/min, and the valve frequency is set at 0.714 Hz to generate 2.8 μL segmentation. Note that there is a ~0.7 min delay in the segmented chromatogram due to the added volume of the segmentation valve and connections. The legend at the right of each chromatogram shows the m/z value for each trace, along with the identity of the corresponding $[M + H]^+$ ion and the full-scale intensity (NL level) for that trace. A zoom-in of the segmented chromatogram over the elution window of 13.5−14.8 min for PC (36:2) and PC (38:4) is shown in Figure S9.

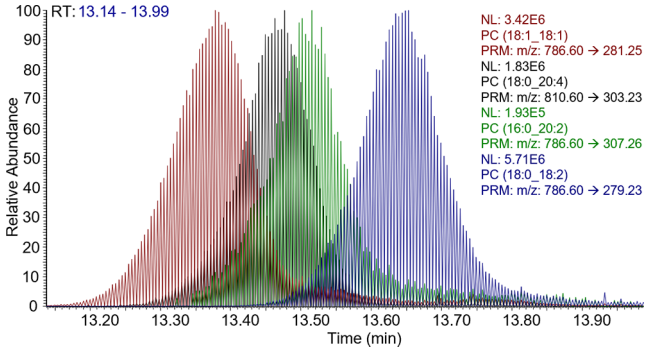

Figure 4. MS/MS data are essential to provide better insight into LC separation of isomers and more informed segment selection for NMR. The extracted specific isomer differentiating the fatty acyl chain fragment ion profile shows four isomers closely eluting over a 0.7 min retention time window. The legend at the right of each chromatogram shows the specific MS/MS transition extracted for each trace, along with the identity of the corresponding $[M + H]^+$ ion and the full-scale intensity (NL level) for that trace.

this problem,[15] we have not yet attempted this surface treatment. Furthermore, the variation in the flow path cross section of the feedlines and flow cell in the Protasis capillary probe induces problems in preserving segmentation integrity during sample transfer. Thus, a dedicated flow probe with low ng sensitivity and the flow path matching the segmented flow storage tubing are desired to couple to the active segmentation platform.

As an alternative for proof-of-concept, here we show that 500 μm i.d. PFA tubing can be used as both the feedline and detection cell in a 10 mm QNP cryoprobe, since neither the PFA tubing nor FC43 contribute to the ^{1}H channel. In addition, no partitioning of protonated LC solvents into FC43 occurs, as shown in Figure 6 (the tubing-through-cryoprobe configuration is depicted in Figure S4). While the current proof-of-concept configuration is far less sensitive compared to the Protasis capillary microcoil probe, it demonstrated that segment isolation is possible if the correct tubing can be incorporated into the design. The loss of sensitivity versus the capillary probe is related to multiple factors: the PFA tubing is very narrow compared to the 10 mm diameter of the probe, shimming could only be partially optimized, and the volume of solvent associated with filling the sensitive volume of the probe was larger, resulting in more Johnson−Nyquist noise in the coil. Note that any appropriate tubing would suffice as long as it was integrated across the LC−MS−NMR platform. Considering that the chromatographic peak apex concentration limit is 10 ng/μL for ESI-MS and that the segments selected for NMR may not be at the chromatogram peak apex, the desired probe sensitivity is in the low ng range. As such, to achieve NMR of a single segment, the sensitivity of the probe needs to increase by the ratio of the concentrations, that is, 15−20 times. This goal is not readily achievable with the

https://doi.org/10.1021/acs.analchem.2c03974
Anal. Chem. 2023, 95, 1908−1915

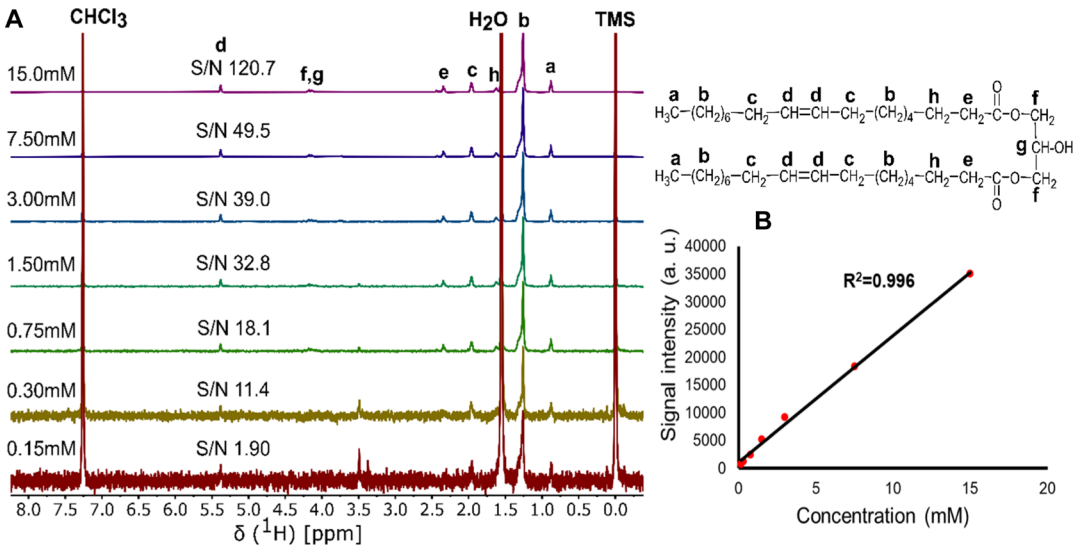

Figure 5. (A) Stacked ^{1}H NMR spectra recorded for *sn*-1,3 diacylglycerol (18:1/18:1) Δ9 trans of different concentration in $CDCl_3$ using the Protasis capillary microcoil probe on a 500 MHz magnet. Concentrations of each sample used to acquire ^{1}H NMR data is noted at the left side of each spectrum. Signal-to-noise (S/N) ratio was calculated for the olefinic signal at δ = 5.3 ppm and displayed on each spectrum. (B) Signal vs concentration of the analyte follows a linear relationship down to the limit of detection.

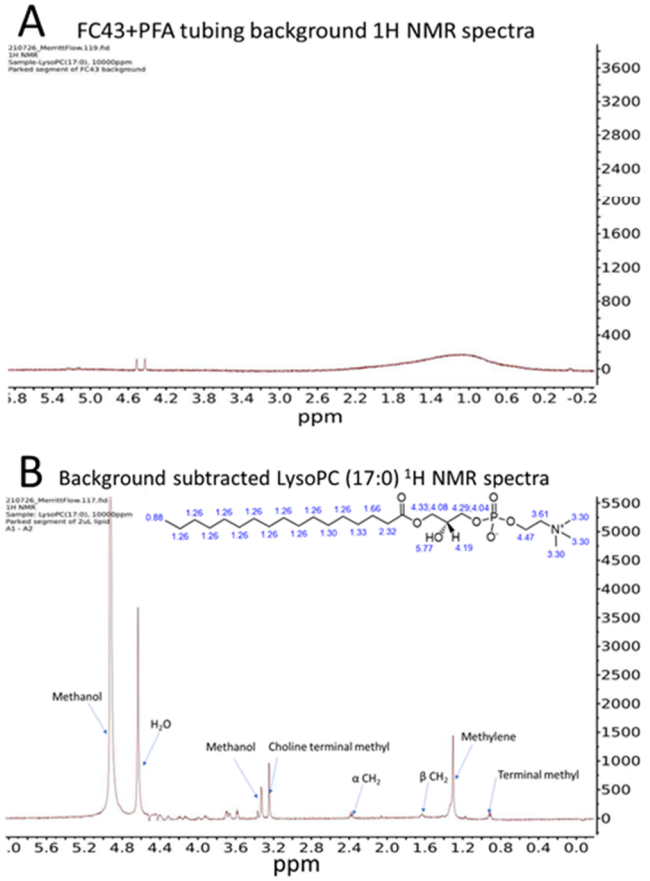

Figure 6. (A) ^{1}H NMR spectrum of PFA tubing filled with FC43, showing that it is transparent under the ^{1}H channel. (B) Background-subtracted ^{1}H NMR spectrum acquired on 2 μL of 10,000 ppm LysoPC (17:0) segment. Major peaks are assigned, and the ChemDraw-predicted ^{1}H NMR chemical shifts are shown at the top for reference. Both spectra are 128 scans to permit baseline subtraction.

current technology. Without considering the probe geometry, the NMR signal scales as $\sim B_o^{3/2}$.[16] Moving from 500 to 800 MHz ^{1}H frequency would improve the sensitivity by ~2 if the microcoil maintained the same efficiency. Unfortunately, modern cryocooled coils for liquid-state NMR are not optimized for samples this small. Currently, the commercial probe with the highest mass sensitivity is the Bruker 1.7 mm probes, but even these systems have detection coil lengths that demand sample volumes of ~30 μL, which again will cause more Johnson−Nyquist noise. To approach "single segment sensitivity," we would need to move to a cryocooled, microcoil design with the PFA tubing as the flow path feedline, preferably at the highest field strength possible. It is not clear that any industry partners are willing to invest in such technology. In our case, independent development of NMR probes, perhaps using high-temperature superconductor technology,[17] is likely the best route for further pursuing this pairing of technologies. In the near term, selecting ~10 segments from the chromatogram would suffice for diagnostic ^{1}H NMR. The NMR signal-to-noise ratio is proportional to (number of scans)^2; if the user wishes to lower the detection limit by a factor of 2, then 256 scans (total experiment time ~25 min) could easily be run. Further signal averaging, for example, overnight, would have to be weighed against the cost and the relative importance of obtaining the absolute lipid ID.

CONCLUSIONS

Herein, we described a practical platform solution to merge NMR into the LC−HRMS/MS-based untargeted lipidomics workflow for absolute lipid structural elucidation. An active segmentation platform targeting analytical LC flow rate was achieved to convert a continuous chromatogram into two parallel segmented flows in the microliter regime, one for real-time MS and MS/MS analysis and the other to be stored for subsequent MS- and MS//MS-guided selection for segments for NMR analysis. MS and MS/MS parameters were optimized for segmented flow, and strategies were developed to retrieve segmentation profile and correlate analytical information. While the platform described is home-built, it could readily

https://doi.org/10.1021/acs.analchem.2c03974
Anal. Chem. 2023, 95, 1908−1915

be adopted by the lipidomics community as all microfluidic components and perfluorinated oil are commercially available, ensuring standardization in implementing the hardware platform across different laboratories. The range of available tubing and valve body dimensions allow the parallel segmentation platform to be scalable across different flow rate regimes to meet different analytical instrumentation and application needs. Our results indicate that a new generation of NMR flow probes could effectively be coupled into an LC−MS−NMR approach, but the choice of tubing must be matched to that used for the LC separation. In addition to innovations in the NMR probe design to optimize the analysis of the stored segmented chromatogram, there are a number of other future directions planned for this work. One is to evaluate options for "rewinding" the stored segmented chromatogram to allow specific segments to be selected for NMR analysis. Another would be dynamic regulation of flow resistance to address the expected increase during segmented flow accumulation within the storage tubing. As for whether to use an aprotic solvent for the LC run so the eluent is directly compatible with NMR analysis, the benefits of using 1.5 mm i.d. columns will be explored as lower flow rates may make use of deuterated solvents affordable.[18] These steps will help improve the platform introduced here for merging NMR into LC−MS based lipidomics workflows.

■ ASSOCIATED CONTENT

Supporting Information

The Supporting Information is available free of charge at https://pubs.acs.org/doi/10.1021/acs.analchem.2c03974.

Valve port connection schematic, effects of TopNddms[2] parameter selection on segmented flow TIC response, egg PC mixture species distribution, egg PC mixture annotated feature lists sorted by retention time, and schematic of PFA tubing through cryoprobe configuration (PDF)

■ AUTHOR INFORMATION

Corresponding Author

Richard A. Yost − *Department of Chemistry, University of Florida, Gainesville, Florida 32611, United States; Department of Pathology, Immunology and Laboratory Medicine, University of Florida, Gainesville, Florida 32610, United States;* orcid.org/0000-0002-1293-5669; Phone: 352-392-0557; Email: ryost@ufl.edu; Fax: 352-392-4651

Authors

Jiajun Lei − *Department of Chemistry, University of Florida, Gainesville, Florida 32611, United States*

Rohit Mahar − *Department of Biochemistry and Molecular Biology, University of Florida, Gainesville, Florida 32610, United States;* Present Address: Department of Chemistry, Hemvati Nandan Bahuguna Garhwal University, Srinagar Garhwal, Uttarakhand-246174, India

Mario C. Chang − *Department of Biochemistry and Molecular Biology, University of Florida, Gainesville, Florida 32610, United States;* orcid.org/0000-0002-2452-2693

James Collins − *Department of Biochemistry and Molecular Biology, University of Florida, Gainesville, Florida 32610, United States*

Matthew E. Merritt − *Department of Biochemistry and Molecular Biology, University of Florida, Gainesville, Florida 32610, United States;* orcid.org/0000-0003-4617-9651

Timothy J. Garrett − *Department of Chemistry, University of Florida, Gainesville, Florida 32611, United States; Department of Pathology, Immunology and Laboratory Medicine, University of Florida, Gainesville, Florida 32610, United States;* orcid.org/0000-0003-1623-009X

Complete contact information is available at: https://pubs.acs.org/10.1021/acs.analchem.2c03974

Notes

The authors declare no competing financial interest.

■ ACKNOWLEDGMENTS

This project was supported by grants from Agilent Technologies, Wellspring Clinical Lab, and the National Institute of Health (R01 grants DK105346, HD087306, DK112865, and DK132254). This study was also supported by the Southeast Center for Integrated Metabolomics (National Institute of Health grant U24 DK097209) and the UF Mass Spectrometry Research and Education Center (supported by NIH S10 OD021758-01A1). A portion of this work was performed in the McKnight Brain Institute at the National High Magnetic Field Laboratory's Advanced Magnetic Resonance Imaging and Spectroscopy Facility, which is supported by National Science Foundation Cooperative Agreement DMR-2128556 and the State of Florida.

■ REFERENCES

(1) Alexandri, E.; Ahmed, R.; Siddiqui, H.; Choudhary, M. I.; Tsiafoulis, C. G.; Gerothanassis, I. P. *Molecules* **2017**, *22*, 1663.

(2) Olson, D. L.; Lacey, M. E.; Sweedler, J. V. *Anal. Chem.* **1998**, *70*, 257A.

(3) Bhatia, A.; Sarma, S. J.; Lei, Z.; Sumner, L. W.UHPLC-QTOF-MS/MS-SPE-NMR: A Solution to the Metabolomics Grand Challenge of Higher-Throughput, Confident Metabolite Identifications. In: Gowda, G.; Raftery, D. (Eds.) NMR-Based Metabolomics. *Methods in molecular biology*, Clifton, N.J., Chapter 7, *2037*, 113−133.

(4) Zhao, Y.; Chen, G.; Yuan, Q. *Am. Inst. Chem. Eng.* **2006**, *52*, 4052−4060.

(5) Garstecki, P.; Fuerstman, M. J.; Stone, H. A.; Whitesides, G. M. *Lab Chip* **2006**, *6*, 437−446.

(6) Xiong, R.; Bai, M.; Chung, J. N. *J. Micromech. Microeng.* **2007**, *17*, 1002−1011.

(7) Nie, J.; Kennedy, R. T. *Anal. Chem.* **2010**, *82*, 7852−7856.

(8) Li, Q.; Pei, J.; Song, P.; Kennedy, R. T. *Anal. Chem.* **2010**, *82*, 5260−5267.

(9) Webb, A. *Anal. Bioanal. Chem.* **2007**, *388*, 525−528.

(10) Hamed, S.; Shay, B.; Basu, A. S.*Capillary Fractionation of HPLC Substrates by a Microfluidic Droplet Generator for High Throughput Analysis. Annual International Conference of the IEEE Engineering in Medicine and Biology Society*, 2011.

(11) Pei, J.; Li, Q.; Lee, M. S.; Valaskovic, G. A.; Kennedy, R. T. *Anal. Chem.* **2009**, *81*, 6558−6561.

(12) Fidalgo, L. M.; Whyte, G.; Ruotolo, B. T.; Benesch, J. L. P.; Stengel, F.; Abell, C.; Robinson, C. V.; Huck, W. T. S. *Angew. Chem., Int. Ed. Engl.* **2009**, *48*, 3665−3668.

(13) Perry, R. H.; Cooks, R. G.; Noll, R. J. *Mass Spectrom. Rev.* **2008**, *27*, 661−699.

(14) Rajski, Ł.; Petromelidou, S.; Díaz-Galiano, F. J.; Ferrer, C.; Fernández-Alba, A. R. *Talanta* **2021**, *228*, 122241.

(15) Kautz, R. A.; Goetzinger, W. K.; Karger, B. L. *J. Comb. Chem.* **2005**, *7*, 14−20.

(16) Levitt, M. H.*Spin Dynamics Basics of Nuclear Magnetic Resonance*, 2nd ed.; Wiley, 2000; p P436.
(17) Johnston, T. L.; Edison, A. S.; Ramaswamy, V.; Freytag, N.; Merritt, M. E.; Thomas, J. N.; Hooker, J. W.; Litvak, I. M.; Brey, W. W. *IEEE Trans. Appl. Supercond.* **2022**, *32*, 1500304.
(18) Fekete, S.; Murisier, A.; Losacco, G. L.; Lawhorn, J.; Godinho, J. M.; Ritchie, H.; Boyes, B. E.; Guillarme, D. *J. Chromatogr. A* **2021**, *1650*, 462258.

https://doi.org/10.1021/acs.analchem.2c03974
Anal. Chem. 2023, 95, 1908−1915